Electric field gradients and impurity distributions in doped noble metals:
A systematic study

I. J. R. Baumvol, M. Behar,* J. A. H. da Jornada, R. P. Livi, K. W. Lodge, A. Lopez Garcia,† and F. C. Zawislak

Instituto de Física, Universidade Federal do Rio Grande do Sul, 90000 Porto Alegre, Brasil

The electric field gradients created at ^{111}Cd nuclei by dilute transition-element impurities in noble metals are studied by the technique of time-differential perturbed angular correlation. The present results supplement previous ones with data for the alloys CuRh, CuPt, AgRh, AgIr, AuRh, AuPd, and AuPt, including temperature and concentration dependence in some typical cases. The results show conclusively that, for most impurities situated to the left of the host noble metals in the Periodic Table, there is a strong attraction between the probe In and the impurity atoms. The binding energy ΔE_B for the probe-impurity system is measured for the CuRh and CuPt alloys. The temperature dependence of the high-frequency quadrupole interaction ν_h due to a single-impurity nearest neighbor to the probe is found to obey the usual empirical law $\nu(T) = \nu(0)(1 - \alpha T^{3/2})$. The wealth of experimental data thus made available allows a systematic examination of the results from which the following facts emerge: (i) The observed high frequency ν_h is related to the nominal valence difference ΔZ between impurity and host and to a parameter λ, the difference in the period of impurity and host in the Periodic Table; (ii) a correlation of ΔE_B with both ΔZ and λ is apparent; and (iii) an inverse correlation between the α parameter and ΔE_B is apparent.

I. INTRODUCTION

In a series of papers we have reported investigations, using the technique of time-differential perturbed angular correlation (TDPAC), of the electric field gradients (EFG) created by different impurity atoms dissolved in the cubic noble metals of Ag[1-3] and Cu.[4] One important result shown by this work is that for impurities located to the left of the Ag and Cu hosts in the Periodic Table, there is a strong enhancement of impurity population nearest neighbor (NN) to the ^{111}In probe atoms. This enhancement, over a random distribution of NN impurities, occurs for the alloys of AgPd,[3] CuPd,[4] and AgPt.[5,6] For the AgPd system with 0.25 at. % of Pd, it was observed that 30% of the probe nuclei feel a high-frequency interaction instead of about 3% which would be expected from a random distribution of impurities. Aided by this strong enhancement we have investigated various other interesting aspects such as the mechanism of population of impurities around the probe atoms, the temperature dependence of the created EFG, dynamical processes at high temperatures and binding energies between impurity and probe atoms and these are reported in the above references.

It now seems important to extend these experiments to include other impurity atoms and also to use the cubic noble metal Au as a host. A systematic study can give additional information concerning the role of the host (the influence of its lattice and electronic structures) as well as the effect of impurities

with different valences on the above-mentioned properties.

In this paper we report the results of the studies of the EFG generated by impurities of Pt and Rh in Cu host, Rh and Ir in Ag host, and Pd, Rh, and Pt in Au host. The temperature dependence of the EFG in the alloys of AgRh, CuRh, and CuPt was also investigated. In one case, AuPd, the concentration of impurity was varied. Table I shows the alloys studied in this paper together with those previously investigated, and also gives the concentration of impurities.

In Sec. II we describe the sample preparation and the data treatment. Section III shows the obtained results. A discussion of the present and previous results is presented in Sec. IV. The most important conclusions are presented in Sec. V.

II. EXPERIMENTAL PROCEDURE

A. Sample preparation

The transition metals used as impurities in this work have high melting points compared to the host noble metals. Due to this the solid solutions were prepared in two steps. First a "mother alloy" of c at. % of the impurity ($0.3 \leq c \leq 8.0$, depending on the impurity solubility in the host[7,8]) with the noble metal was melted in an arc furnace. In a second step, adequate quantities of this alloy and the noble metal were melted in a resistance furnace.

TABLE I. Summary of the investigated alloys (hosts and impurity concentrations).

Host	Impurity	Measured impurity concentration	
		Room temperature (at. %)	Function of temperature (at. %)
Cu	Pd[a]	0.5, 1.0, 1.5, 2.5, 4.5	0.7
	Pt	1.0	1.0
	Rh	0.5	0.5
Ag	Pd[b]	0.25, 0.5, 1.0, 1.5, 2.0, 2.5	0.5
	Rh	0.25, 0.5	0.25
	Ir	0.2	
	Pt[c]	0.3, 1.0	0.3
Au	Pd	0.5, 1.0, 2.0, 3.0, 4.5	
	Rh	0.5	
	Pt	0.5	

[a]Reference 4.
[b]Reference 3.
[c]References 5 and 6.

For the Cu and the Au alloys, the radioactive carrier-free ^{111}In obtained through the reaction ^{109}Ag$(\alpha, 2n)^{111}$In was electroplated on the mother alloy before the second step and for the Ag alloys we used the α-irradiated Ag directly.

All the samples were melted in argon atmosphere, and annealed, also in argon, for some hours at 800 °C. The purity of the component metals was $\geq$ 99.99%. This means that our samples contain three elements, the host, the solute impurity atoms, and the very dilute carrier-free, radioactive atoms of ^{111}In, which decay to ^{111}Cd.

B. Data treatment

The TDPAC experiments were performed using the 173−247-keV γ-γ cascade in ^{111}Cd, to measure the hyperfine interaction of the nuclear quadrupole moment of the 247-keV state with the EFG generated at the probe nucleus by the impurity.

The TDPAC data were analyzed in the usual way.[9] From the measured coincidence counting rates at angles of 90° and 180°, the ratio

$$C(t) = 2\frac{C(180°,t) - C(90°,t)}{C(180°,t) + 2C(90°,t)} = A_{22}G_{22}(t) \qquad (1)$$

was calculated, after corrections for random coincidences and misalignment of the sample. The perturbation factor

$$G_{22}(t) = \sigma_{20} + \sum_{n=1}^{3} \sigma_{2n}\cos(\omega_n t)\exp(-\tfrac{1}{2}\delta\omega_n t) \qquad (2)$$

contains the information about the nuclear quadrupole interaction in the frequencies ω_n. These specify the nuclear quadrupole frequency, ν_Q, and the asymmetry parameter, η,

$$\nu_Q = eQV_{zz}/h, \quad \eta = (V_{xx} - V_{yy})/V_{zz} . \qquad (3)$$

Here V_{zz}, V_{yy}, and V_{xx} are the usual principal components of the EFG, and Q is the quadrupole moment of the 247-keV state in ^{111}Cd. The term $\exp(-\tfrac{1}{2}\delta\omega_n t)$ in expression (2) accounts for the Lorentzian distribution of frequencies having a width δ.

In all cases it was observed that a part (a_h) of the probe nuclei are subjected to high-frequency interactions ν_h, a second part (a_l) to a distribution of low frequencies centered around ν_l, and a third part (a_0) do not feel any hyperfine interaction. Adequate computer fittings were performed using expression (2) in order to extract the amplitudes and the corresponding frequencies from each $A_{22}G_{22}(t)$ curve.

III. RESULTS

Typical results for the perturbation factor $A_{22}G_{22}(t)$ are shown in Figs. 1−3. The full lines in the figures show the computed least-squares fittings. The parameters obtained from the fittings are displayed in Tables II−IV.

In particular, the results shown in Table II are for the lowest measured concentration of impurity in each alloy, including the data from our previous experiments for AgPd (Ref. 3) and CuPd (Ref. 4) as
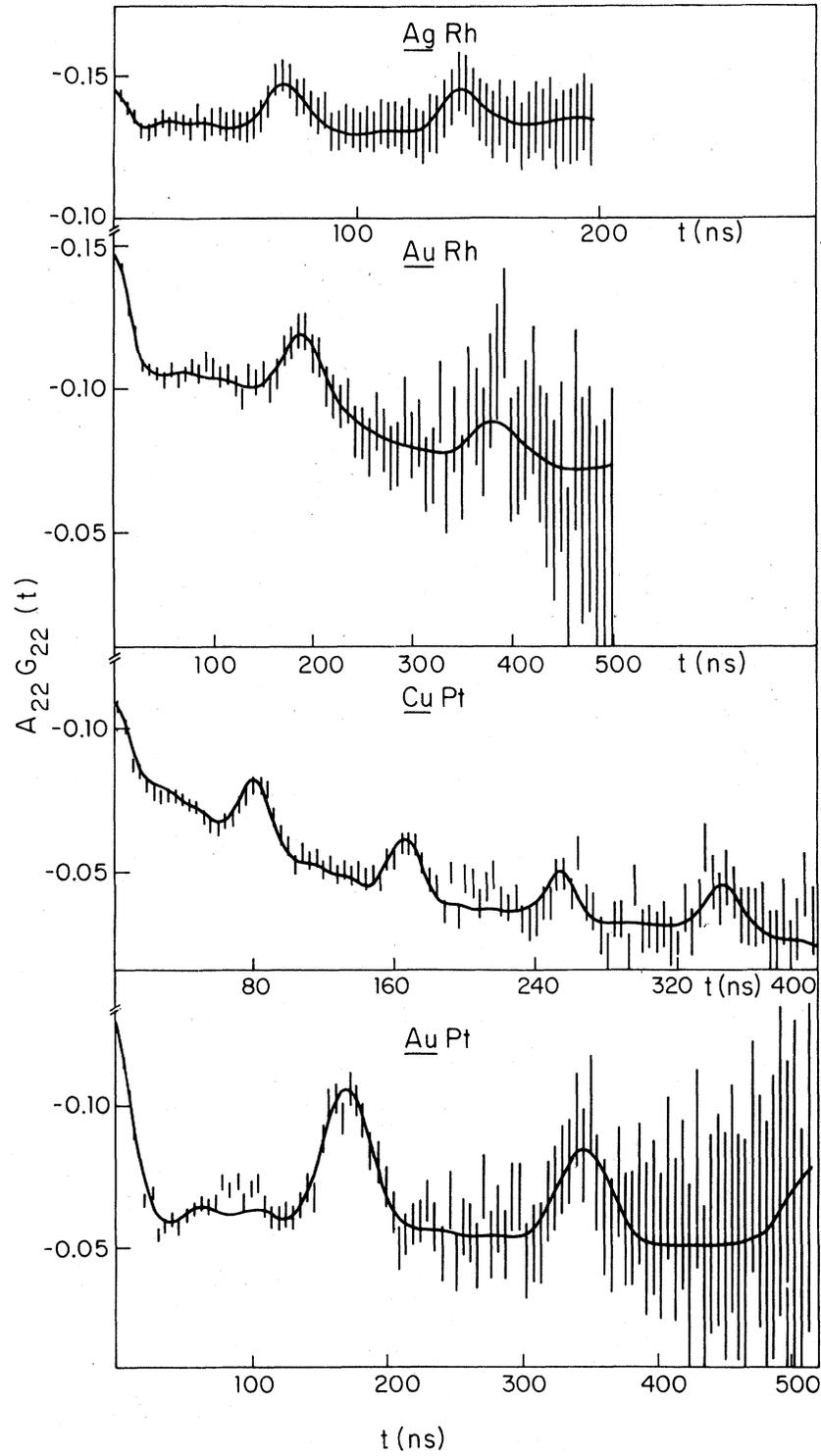
FIG. 1. Typical $A_{22}G_{22}(t)$ spectra for various alloys. The full lines are computer least-squares fittings.
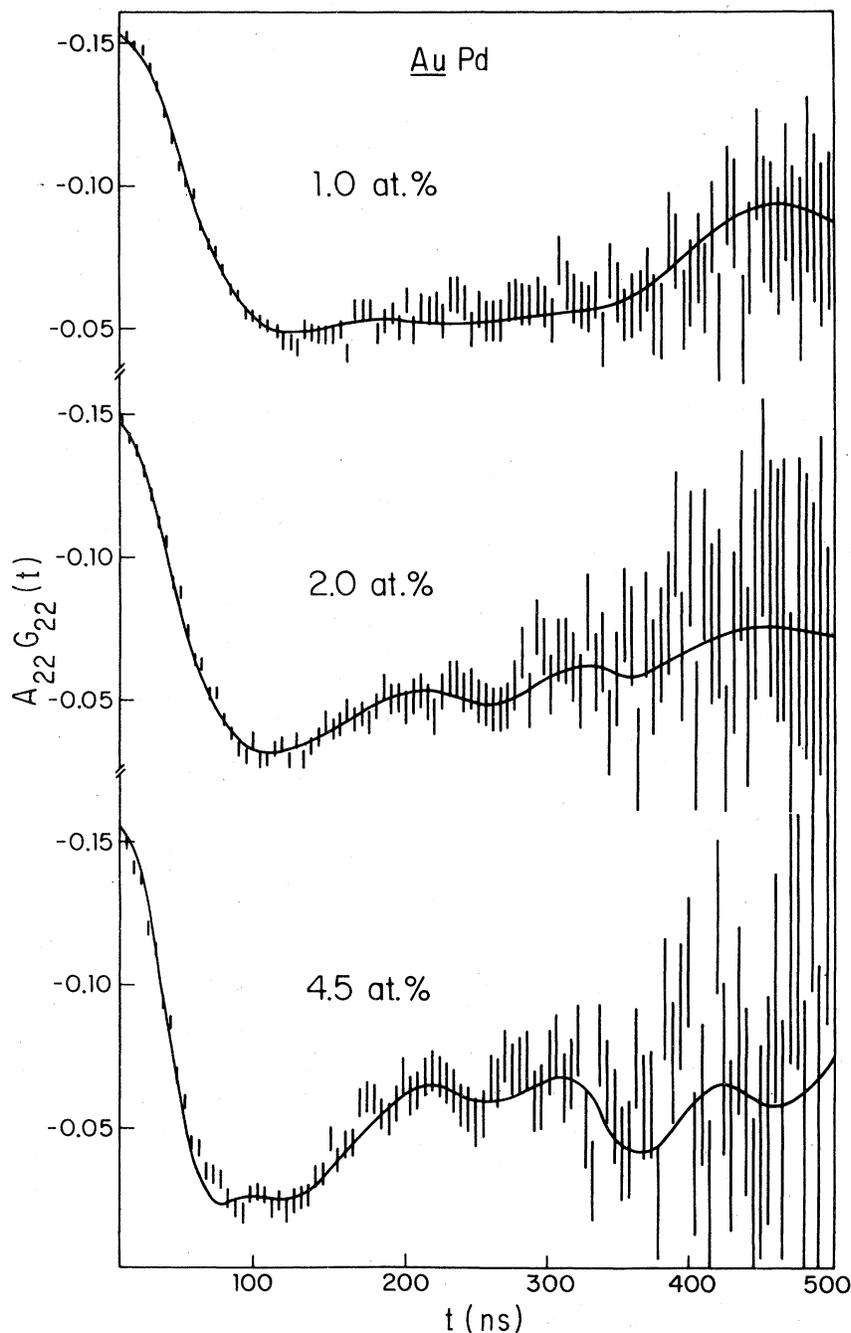
FIG. 2. $A_{22}G_{22}(t)$ curves for three concentrations of Pd in Au host. The full lines are computer least-squares fittings.

well as the results for AgPt.[5,6]

Figure 2 shows typical $A_{22}G_{22}(t)$ results at various impurity concentrations in AuPd. The extracted parameters are shown in Table III for impurity concentrations in the range 0.5–4.5 at. %.

Figure 3 shows typical $A_{22}G_{22}(t)$ results at various temperatures in CuRh with 0.5 at.% Rh. Table IV displays the results of the temperature-dependence

study for the alloys of AgRh (0.25 at. %), CuRh (0.5 at. %), and CuPt (1.0 at. %).

A. Concentration dependence

For two of the investigated alloys, AuPd and AgRh, the concentration of impurity was changed.
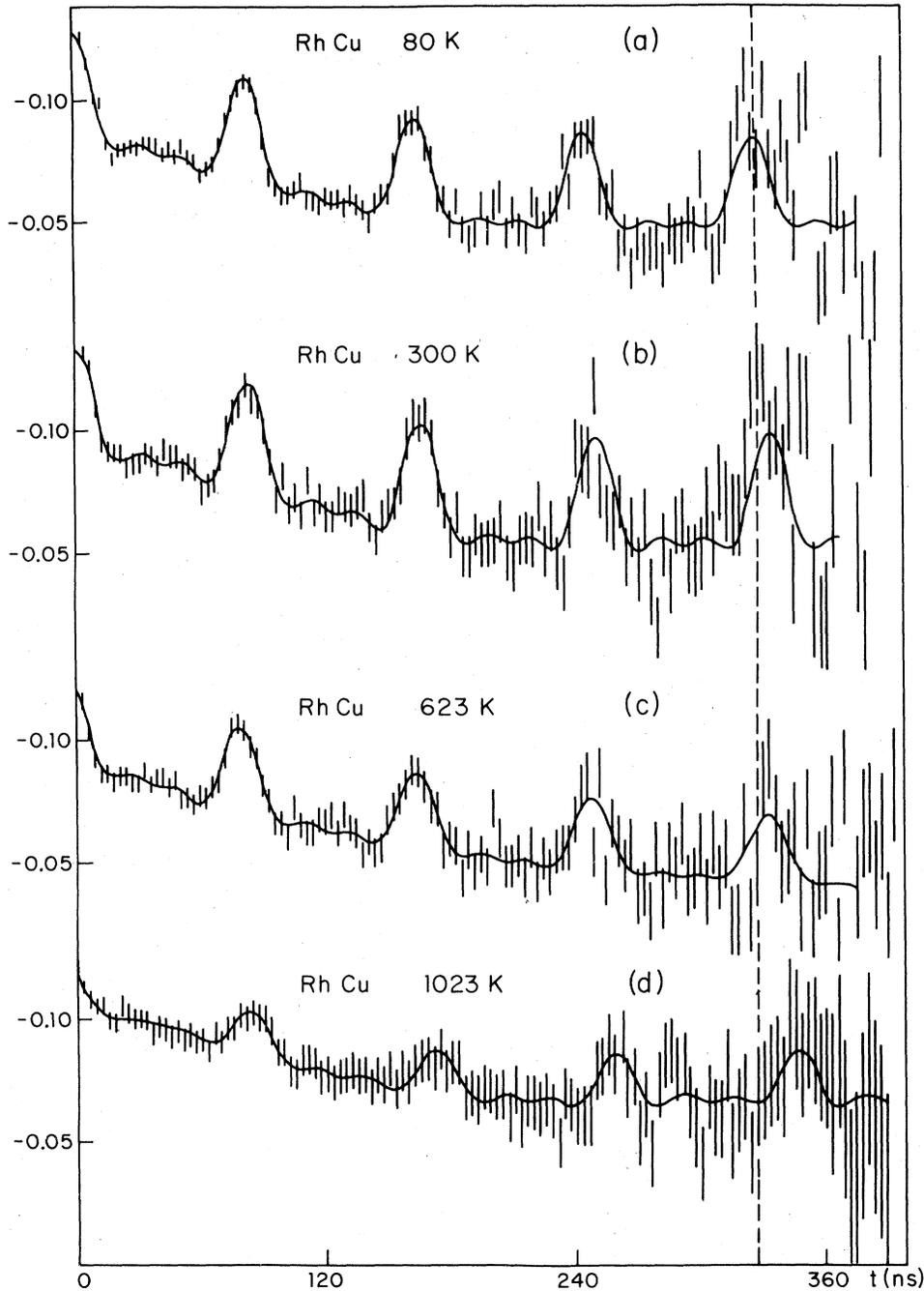
FIG. 3. $A_{22}G_{22}(t)$ curves for 0.5 at.% of Rh impurity in Cu, measured at different temperatures.

Since the available information in the literature[8] indicates that the solubility of Rh in Ag is small, we measured the EFG only for concentrations of 0.25 and 0.5 at.%. The computer fitting of the $A_{22}G_{22}(t)$ curves gave the same parameters for both concentrations. Figure 1 shows the result for 0.25 at.% of concentration and the extracted parameters are in Table II. The observation that the amplitudes and

the frequencies are the same for both concentrations indicates that there is a segregation of the impurity. This fact is confirmed by the lack of any low-frequency interaction (due to distant neighbors to the probe), in opposition to what is observed for all other impurities. Very likely the segregation starts at lower concentrations than 0.25 at.%.

The Au Pd results are displayed in Table III. As

TABLE II. Quadrupole interaction frequencies, with their respective amplitudes and distributions, for several alloys with the lowest concentration of impurity (see Table I). The errors on the amplitudes a are typically 10%.

System	Impurity Concentration (at. %)	a_0	a_l	ν_l (MHz)	δ_l	a_h	ν_h (MHz)	δ_h
CuPd[a]	0.5	0.08	0.64	2.63 ± 0.20	0.50 ± 0.10	0.28	52.8 ± 0.5	0.01
$\cdot Cu$Pt	1.0	0.23	0.56	6.2 ± 0.6	0.50 ± 0.10	0.21	80.2 ± 0.8	0.01
CuRh	0.5	0.27	0.37	6.6 ± 0.5	0.15 ± 0.02	0.36	80.2 ± 0.8	0.01
AgPd[b]	0.25	0.65	0.05	6.66 ± 0.67	0.40 ± 0.04	0.30	43.6 ± 0.9	0.01
AgRh	0.25	0.91	$\cdots$	$\cdots$	$\cdots$	0.09	75.1 ± 1.0	0.01
AgIr[c]	0.2	0.51	0.46	2.9 ± 0.4	0.30 ± 0.10	0.03	201.0 ± 6.0	0.01
AgPt[d]	0.3	≈ 0.50	≈ 0.15	0	$\cdots$	≈ 0.38	76.5 ± 0.8	$\cdots$
AuPd	0.5	0.22	0.14	0.80 ± 0.10	0.22 ± 0.04	0.64	14.1 ± 1.0	0.15 ± 0.02
AuPt	0.5	0.46	0.07	3.9 ± 0.2	0.29 ± 0.04	0.47	38.9 ± 0.5	0.04 ± 0.01
AuRh	0.5	0.50	0.22	3.6 ± 0.6	0.10 ± 0.02	0.28	35.7 ± 0.5	0.06 ± 0.02

[a]From Ref. 4.
[b]From Ref. 3.
[c]Preliminary results.
[d]Amplitudes estimated from Ref. 6.

with the previously reported experiments for AgPd and CuPd, we see the onset of new high frequencies as the impurity concentration is increased. At 0.5 at. % two frequencies are present, one very low, $\nu_l = 0.8$ MHz, with 22% of distribution and a second one, ν_h^1, 20 times larger with a similarly large distribution of 15%. When the concentration is increased, the low frequency disappears, the distribution of ν_h^1 decreases to 1% and two new sharp frequencies ν_h^2 and ν_h^3, larger than ν_h^1 appear. In accordance with the interpretation given in Ref. 3, the frequency ν_h^1 is due to one NN impurity atom, the frequencies ν_h^2 and ν_h^3 are generated by different configurations of two NN impurities and the smeared-out low-frequency ν_l comes from impurities located at larger than NN distances from the probe nucleus. The amplitudes of the high frequencies are strongly enhanced over a

random distribution of impurities, showing again the presence of a strong attraction between the In probe and the Pd-impurity atoms. For 0.5 at. % of impurity the enhancement factor f_h of the amplitude for the high frequency is of the order of 10.

B. Temperature dependence

The effect of temperature on the EFG was measured for the three alloys, CuRh (0.5 at. %), CuPt (1.0 at. %), and AgRh (0.25 at. %). The results are shown in Table IV. For each alloy the high-frequency quadrupole interaction follows the empirical $T^{3/2}$ temperature dependence[10]:

$$\nu(T) = \nu(0)(1 - \alpha T^{3/2}) \ . \tag{4}$$

TABLE III. Parameters extracted from the fitting of $A_{22}G_{22}(t)$ curves for different concentrations of Pd impurity in Au matrix at room temperature. (The fitting for ν_l and ν_h^1 gave $\eta = 0$. Typical errors are 10% for ν_l, δ, and η, 7% for ν_h, and 10% for a.)

C (at. %)	a_0	a_l	ν_l (MHz)	δ_l	a_h^1	ν_h^1 (MHz)	δ_h^1	a_h^2	ν_h^2 (MHz)	δ_h^2	η_h^2	a_h^3	ν_h^3 (MHz)	δ_h^3	η_h^3
0.5	0.22	0.14	0.8	0.22	0.64	14.1	0.15	$\cdots$	$\cdots$	$\cdots$	$\cdots$	$\cdots$	$\cdots$	$\cdots$	$\cdots$
1.0	0.30	$\cdots$	$\cdots$	$\cdots$	0.70	14.3	0.13	$\cdots$	$\cdots$	$\cdots$	$\cdots$	$\cdots$	$\cdots$	$\cdots$	$\cdots$
2.0	0.25	$\cdots$	$\cdots$	$\cdots$	0.45	14.8	0.06	0.30	19.8	0.05	0.45	$\cdots$	$\cdots$	$\cdots$	$\cdots$
4.5	0.20	$\cdots$	$\cdots$	$\cdots$	0.20	15.4	0.01	0.38	20.2	0.05	0.45	0.22	26.3	0.05	0.40

TABLE IV. Parameters extracted from the temperature dependence of the EFG for the CuRh, CuPt, and AgRh systems. (The typical errors are 10% for a_0, a_l, and a_h, 20% for ν_l and δ_l, and 1% for ν_h.)

	T (K)	a_0	a_l	ν_l (MHz)	δ_l	a_h	ν_h (MHz)
	80	0.33	0.32	6.8	0.3	0.35	81.9
	300	0.27	0.37	6.6	0.15	0.36	80.2
	523	0.15	0.53	3.7	0.61	0.32	79.2
	573	0.18	0.54	3.0	0.95	0.28	79.0
CuRh							
	623	0.18	0.57	3.0	0.97	0.25	79.5
	723	0.18	0.60	3.2	0.8	0.22	76.8
	873	0.38	0.44	5.9	0.5	0.18	75.7
	1023	0.55	0.30	6.7	0.27	0.15	75.1
	80	0.22	0.57	6.01	0.5	0.21	81.5
	300	0.23	0.56	6.2	0.5	0.21	80.2
	573	0.41	0.38	9.79	0.21	0.21	79.0
	673	0.36	0.46	8.67	0.25	0.19	79.8
CuPt							
	773	0.32	0.51	7.86	0.38	0.17	77.6
	873	0.20	0.64	5.80	0.62	0.16	76.2
	973	0.26	0.59	4.98	0.70	0.15	75.7
	1023	0.16	0.71	4.15	0.60	0.13	75.0
	80	0.91				0.09	76.0
	300	0.91				0.09	75.1
AgRh							
	523	0.90				0.10	73.8
	673	0.90				0.10	73.2

TABLE V. Enhancement factors f_h and F_h and parameters α, ΔE_B, and T_0 obtained from temperature experiments for various alloys.

Alloy	Impurity concentration[a] (at. %)	f_h	α (10^{-5} K$^{-3/2}$)	ΔE_B (meV)	T_0 (K)	F_h	$\ln F_h$	$\dfrac{\Delta E_B}{kT_0}$	$\dfrac{\alpha \Delta E_B}{}$ (10^{-8} eV K$^{-3/2}$)
CuPt	1.0	1.8	0.25 ±0.02	60±15	620	2.2	0.79	1.12	15±4
CuPd[b]	0.5	4.7	0.31 ±0.05	100±40	600	6.4	1.9	1.9	31±14
CuRh	0.5	6.0	0.29 ±0.02	86±8	430	9.3	2.2	2.3	25±3
AgPd[c]	0.25	10	0.18 ±0.04	122±20	710	14	2.7	2.0	22±6
AgPd[d]	0.3	≈9	0.203±0.025	135±9	≈570	≈13	≈2.6	≈2.7	27±4
AgPt[d]	0.3	≈10	0.176±0.011	171±9	≈600	≈17	≈2.8	≈3.3	30±3

[a]Concentration for which f_h, F_h, and $\ln F_h$ are calculated. In principle only f_h is concentration dependent.
[b]Reference 4.
[c]Reference 3.
[d]References 5 and 6. The values of T_0 are from the crossing points in Fig. 2 of Ref. 6.

The extracted α coefficients from the fittings are shown in Table V, which also includes results from previous measurements.

The CuRh and CuPt systems were studied in the temperature range from 80 to 1023 K. As well as the change of the quadrupole frequency, Table IV also shows that, for these two alloys, the amplitude a_h of the high frequency decreases at high temperatures. Simultaneously the sum of the amplitude $a_0 + a_l$ (background plus low-frequency amplitudes) increases in the same temperature range. We associate the high frequency with bound In-impurity pairs (InX), the impurity being NN to the probe In atom, and these have a fractional population a_h. For the remainder of the population $(a_0 + a_l)$, the In probe atoms have the impurity beyond the NN, feel a low-frequency interaction or none at all, and are represented by (In + X). Our data show that, as the temperature increases we have the chemical reactions (InX) $\rightleftharpoons$ (In + X), with the net result that at 1023 K about 50% of the (InX) bound pairs present at 80 K were broken and transformed into distant neighbors. The measured amplitude variation with temperature was found to be independent of the order of the different temperature runs using an average rate of change of temperature between runs of about 10^{-2} K s^{-1}, and run times of the order of 12 h.

The data of Table IV allow the determination of the difference in binding energy ΔE_B, between the systems (InX) and (In + X), for $X =$ Rh, Pt in a Cu host. Assuming the validity of the law of mass action and neglecting entropy effects, we can write

$$\ln \frac{a\,(\text{In}X)}{a\,(\text{In}+X)} = \ln \frac{a_h}{a_0 + a_l} = \frac{\Delta E_B}{kT} \quad . \tag{5}$$

Figure 4 shows the experimental values of $a_h / (a_0 + a_l)$ plotted on a logarithmic scale against T^{-1}. In the high-temperature region the data are fit-

ted very well by a straight line. Up to about 430 K in CuRh and about 620 K in CuPt, the impurity and probe atoms are not mobile and for these temperatures Eq. (5) is not obeyed. The results obtained for the difference in binding energy ΔE_B are 86 ± 8 meV in CuRh and 60 ± 15 meV in CuPt. These are compared in Table V with previous measurements in other doped alloys.

For the AgRh alloy, the EFG also follows the $T^{3/2}$ law but the amplitudes are constant at least up to 673 K, the highest measured temperature. With the present data we cannot discriminate between a normal detrapping process for AgRh, but beginning above 673 K, or a process where detrapping is compensated by some means.

IV. DISCUSSION OF SYSTEMATIC TRENDS

A. Impurity-probe interaction

Table II shows the frequencies, amplitudes, and distributions obtained at lowest measured impurity concentration for the various alloys studied in this paper and in previous work. All the impurities are to the left of the noble-metal hosts in the Periodic Table and in each case there is only one high frequency ν_h which is associated with one impurity atom NN to the probe. For nine of the ten alloys listed, the exception being AgIr, there is a strong enhancement of NN populations over that expected from a random distribution of impurities. This signifies an attraction between the In probe and the impurity atoms. The enhancement factor f_h $(= a_h/12c'$ where c' is the fractional impurity concentration) ranges from 2 in CuPt to about 10 in AgPd, AgPt, and AuPd. We shall also see that the apparent exception AgIr fits into a scheme of varying enhancement for the different impurity and host combinations.
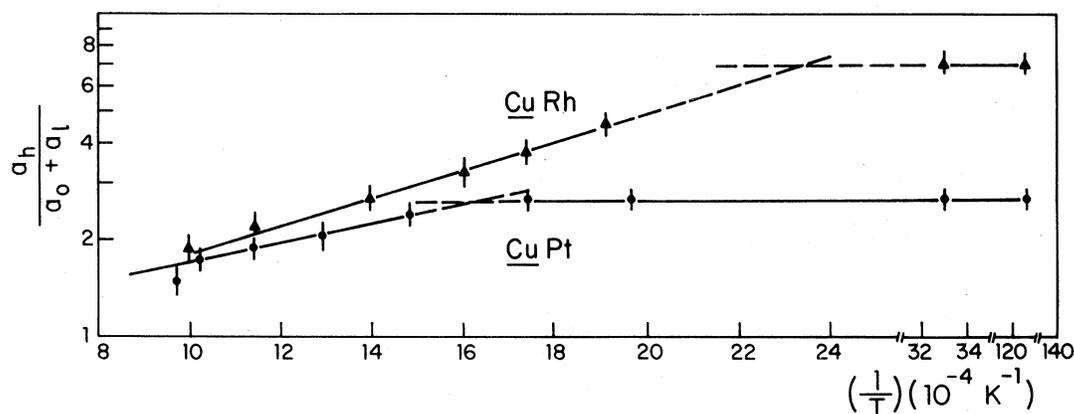
FIG. 4. Experimental values of $a_h/(a_0 + a_l)$ on a logarithmic scale vs $1/T$ for CuRh and CuPt. The lines show the linear fittings (see text).

For those alloys where temperature effects have been measured, there is, as might be expected, a rough correlation between the enhancement factor f_h and the binding energy ΔE_B. Table V shows that high f_h is associated with high ΔE_B. A more precise relationship between these two quantities can be obtained after including the neglected entropy effects in Eq. (5). If the system is in thermodynamic equilibrium

$$\ln\left[\frac{a_h}{a_0 + a_l}\right] = \frac{\Delta E_B}{kT} + \frac{1}{k}\Delta S \ , \tag{6}$$

where ΔS is the difference in configurational entropy between the state with one impurity NN to the probe and the state with no impurity NN to the probe.

Our enhancement factors apply at low temperatures where the alloys are not in thermodynamic equilibrium. Instead, constant values of the amplitudes were obtained. If we define T_0 as the temperature of intersection of the low- and high-temperature lines in Fig. 4 then the low-temperature amplitudes obey

$$\ln\left[\frac{a_h}{a_0 + a_l}\right] = \frac{\Delta E_B}{kT_0} + \frac{1}{k}\Delta S \ . \tag{7}$$

T_0 indicates the temperature region where transformation between the high-temperature equilibrium situation and the low-temperature frozen situation occurs. It could in principle be related to the thermal treatment of the sample and impurity diffusion rates.

If no more than one impurity NN to the probe is observed $(a_0 + a_l + a_h = 1)$, the left-hand side of Eq. (7) becomes $\ln[a_h/(1 - a_h)]$ and a relationship between the enhancement factor and the binding energy immediately results. Where configurations with more than one impurity NN to the probe occur, the one NN impurity amplitude (a_h) can conveniently be renormalized to $a_h' = a_h/(a_0 + a_l + a_h)$, giving the left-hand side of Eq. (7) as $\ln[a_h'/(1 - a_h')]$. The simplest approximation for evaluating the entropy term in Eq. (7) is to allow all possible arrangements of one In probe atom and $c'N$ impurity atoms on the N lattice sites of the crystal. Then, neglecting surface effects,

$$\frac{1}{k}\Delta S = \ln\left[\frac{12N(N-13)!/(c'N-1)!(N-c'N-12)!}{N(N-13)!/(c'N)!(N-c'N-13)!}\right]$$

$$= \ln[12c'/(1-c')] \tag{8}$$

for large N.

Thus, the modified enhancement factor F_h, defined by

$$F_h = \frac{a_h'/(1 - a_h')}{12c'/(1 - c')} \ , \tag{9}$$

is related to the binding energy by

$$\ln F_h = \Delta E_B/kT_0 \ . \tag{10}$$

F_h is the ratio of observed to randomly distributed populations for one impurity NN to the probe, each being expressed relative to the populations for no impurity NN to the probe.

The experimental results have been analyzed on this basis in Table V. There is a very good comparison between $\ln F_h$ and $\Delta E_B/kT_0$, much better than the rough correlation between f_h and ΔE_B. The data from Refs. 3 and 6 for AgPd are treated separately because of differences in sample treatments. The less satisfactory comparison for the Ref. 3 results is most probably due to the quenching used being too slow, resulting in an unnaturally high T_0.

The plausibility of the obtained values of T_0 can be checked using known impurity diffusion constants and the sample treatment. In our experiments the samples spent typically 3 h at measurement temperature before and in the early part of the temperature runs. Allowing several jumps for either the probe In or the transition-metal impurity to occur in this time we estimate that a minimum jump rate of 10^{-3} s^{-1} is required to establish equilibrium for the bulk of the measurement period. The only case where both In and impurity diffusion constants in the host metal are known is AgPd and here In is the most mobile giving a temperature of 510 K for the above jump rate. This is in reasonable agreement with the preferred value for T_0 of 570 K, although, since this is obtained from Ref. 6, the required jump rate is uncertain. Fortunately the calculated temperature depends only weakly on the minimum jump rate, a change by a factor of 10 in the jump rate producing only a 5% change in the temperature. In addition, the above treatment must be viewed as an approximation since it assumes that the measured tracer diffusion rates are valid in the presence of the impurity-probe interaction.

With the In diffusion identified as responsible for the value of T_0 in AgPd, the value of T_0 in AgPt is expected to be the same or lower. Although the values in Table V show the reverse of this the difference is small. Also the low value of T_0 in CuRh compared to the other two Cu alloys indicates that there the diffusion of Rh is the important factor.

The obvious quantity to use in a systematic study of the probe-impurity interaction in the various alloys is the binding energy ΔE_B. Since it has been determined for only one-half of the studied alloys, it is estimated for the others using the measured low-temperature amplitudes and Eq. (10). This involves an estimation of the temperature T_0 which is set at 600 K from the indications of Table V, unless there is evidence to the contrary. This value probably has an uncertainty of at most 30%. For AgRh the amplitude a_h was found to be constant up to 673 K and we have set T_0 for this alloy at 700 K.

Trends between measured binding energies and EFG effects are discussed in Sec. IV B and trends

among binding energies, including estimated values, are analyzed in Sec. IV C.

B. Electric-field-gradient behavior

The room-temperature values of the high-frequency ν_h for all the alloys are analyzed in Sec. IV C on the basis of host and impurity position in the Periodic Table.

For alloys where temperature effects have been measured the high-frequency ν_h follows the empirical $T^{3/2}$ temperature dependence [Eq. (4)]. This strongly suggests that the cause of the EFG temperature dependence in dilute cubic alloys is the same as in noncubic metals, arising from the thermal vibrations of the atoms.[11-13] This idea is further strengthened by an apparent correlation between the binding energy and the α parameter which gives the strength of the temperature dependence. If the temperature dependence of the EFG is governed by thermal vibrations, for strongly bound systems (higher binding energy) one would expect a smaller temperature dependence of the EFG. This fact is confirmed experimentally; the values of the α parameter are smaller for strongly bound probe-impurity pairs and larger for weakly bound pairs. This correlation can be observed more clearly from the product $\alpha \Delta E_B$ listed in Table V which, with the possible exception of the CuPt alloy, is approximately constant while ΔE_B varies by a factor of about 2.

It should be emphasized that the probe-impurity interaction of importance to the value of α applies to the situation when the probe is ^{111}Cd, whereas the measured binding energies apply to the situation when the impurity population is in thermodynamic equilibrium and the probe is still ^{111}In. Therefore, in making the preceding argument connecting α and ΔE_B we must assume that the measured In-impurity binding energies give a measure of the Cd-impurity binding energies. Furthermore, within the vibrating-atom picture of the temperature dependence, one really expects that α should depend in some manner on the hardness of the potentials seen by the vibrating atoms contributing to the observed EFG and also on the masses of these atoms.[14] Though it is natural to expect the hardness of a potential to be related to its depth, a description of α just in terms of the binding energy of the one NN impurity configuration can be expected to give only qualitative agreement at best. An improvement would be to use α values with the mass effects eliminated, but current theory[15] is only applicable to the Ag alloys where the probe and host atoms are of similar mass. It is interesting that this theory predicts a decrease in α for large impurity to host mass ratio, in line with the exceptionally small $\alpha \Delta E_B$ in CuPt where the mass ratio is largest.

A further trend involving α values and binding can be seen on comparing the temperature dependence of the high and low frequencies, due, respectively, to NN and distant neighbors. For the high frequencies, associated with strongly bound probe-impurity pairs, α is in the range $0.2-0.3 \times 10^{-5}$ K$^{-3/2}$ (Table V). The low-frequency distributions have a much stronger temperature dependence, with α an order of magnitude larger. In the AgPd alloy[3] the low smeared-out frequency had α as $(3.1 \pm 0.6) \times 10^{-5}$ K$^{-3/2}$. From the data of Table IV similar values can be obtained for CuRh in the range 80–700 K and for CuPt in the range 600 to 1000 K. This failure of the low-frequency distribution to hold to the $T^{3/2}$ dependence throughout the complete temperature range may be due to thermal changes in the distribution of impurities between different non-NN shells.

We do not suggest that the reciprocal relation between α and binding energy, evidenced for the NN impurity interaction, also holds for comparing NN and non-NN impurity interactions. Obviously for a very distant impurity, where impurity-probe binding is negligible, the associated EFG would be expected to have a temperature dependence governed by the independent vibration of the probe and the impurity relative to the host. However the trend of decreasing α with increasing impurity-probe binding is apparent and supports the interpretation of the EFG temperature dependence as arising from the thermal vibrations of the atoms.

In connection with the above discussion it is interesting to note that for the AgPd alloy[3] the high frequency generated by one NN impurity of Pd had a weaker temperature dependence [$\alpha = (0.18 \pm 0.04) \times 10^{-5}$ K$^{-3/2}$] than the frequency due to two NN of Pd [$\alpha = (0.44 \pm 0.10) \times 10^{-5}$ K$^{-3/2}$]. It seems that in this alloy each impurity in the two NN configuration is bound more weakly (to the probe atom) than in the configuration of one NN, perhaps due to the repulsion between impurities.

C. Periodic Table analysis

In the following we analyze the high-frequency data of Table II and the binding-energy results of Table V in terms of the valence difference between impurity and host, size effects and quantum numbers of the last d shell of hosts and impurities. Since the valence of a transition-metal ion in a metallic environment is not obvious we take the valence as that used in the transition-metal model potential of Animalu.[16] Such potentials are applicable in principle to a theoretical treatment of the systems under study.

We thus have the following assumptions: (i) There is an effective difference of valence between impurity and host [$\Delta Z = Z(\text{impurity}) - Z(\text{host})$] of

TABLE VI. High frequencies ν_h and binding energies ΔE_B for the measured alloys arranged as function of valence difference and atomic period.

	Impurity	Host	λ	Alloy	$\Delta Z = 1$ ν_h (MHz)	ΔE_B (meV)	Alloy	$\Delta Z = 2$ ν_h (MHz)	ΔE_B (meV)	Alloy	$\Delta Z = 3$ ν_h (MHz)	ΔE_B (meV)
	4d	5d	−1	AuPd	14	175[a]	AuRh	36	96[a]			
	4d	4d	0	AgPd	44	135±9	AgRh	75	72[a]			
Ag- and Au-based alloys	5d	5d	0	AuPt	39	139[a]						
	5d	4d	1	AgPt	76	171±9				AgIr	201	13[a]
Cu-based alloys	4d	3d	1	CuPd	53	100±40	CuRh	80	86±8			
	5d	3d	2	CuPt	80	60±15						

[a]Estimated using Eq. (10) (see text) and probably in error by at most 30%. Some uncertainty exists for the effective concentration (≤ 0.25 at. %) in the AgRh alloy.

$\Delta Z = 1$ for Pd and Pt, $\Delta Z = 2$ for Rh, and $\Delta Z = 3$ for Ir. The value of $Z = 4$ for Ir is justified in Ref. 16.
(ii) We define a parameter λ as the difference between the principal quantum numbers of the last d shell of the impurity and host atoms. In this way λ will parametrize the effects of period in the Periodic Table. (iii) Because Ag and Au have similar atomic volumes and electronic band structures we shall compare and correlate the results for both hosts. The host of Cu has a different atomic volume and band structure; the Cu-based alloys will be analyzed separately.

The high-frequency interaction ν_h and the corresponding binding energy ΔE_B are presented in Table VI for the various alloys and classified according to the above considerations. Also included are estimates of the binding energy as described in Sec. IV A for those alloys where ΔE_B was not measured.

The following facts emerge from an analysis of Table VI. (a) Independent of impurity and host, there is an increase of the frequency ν_h and an apparent decrease of the binding energy ΔE_B with increasing ΔZ. (b) There is a correlation between the frequencies and the period parameter λ. The data for $\Delta Z = 1$ show clearly that when λ increases the frequency also increases. In addition, with the exception of AgPt, a decrease in ΔE_B with increasing λ is apparent. (c) The frequencies for the impurities of Pd, Rh, and Pt in Cu host are systematically higher than in the other two hosts. This increase can be attributed, at least in part, to the fact that in the Cu host the distance between impurity and probe atoms is smaller than in the other two hosts.

From the correlation between ΔE_B and ΔZ we see that the lack of enhancement in AgIr is not really an exceptional case, but fits naturally into a scheme of

decreasing binding energy with increasing valence difference between impurity and host.

The increase of the high frequency with a positive nominal charge difference ΔZ was observed previously in TDPAC work with a Ag host[1] and also in NMR work with a Cu host,[17] though in the latter case a saturation effect is apparent for high ΔZ. Table VI shows that from $\Delta Z = 1$ to $\Delta Z = 2$, on the average the high frequencies double in value and for AgIr ($\Delta Z = 3$), the frequency is three times larger than that for AgPt ($\Delta Z = 1$).

V. CONCLUSIONS

The present results together with those of previous experiments show conclusively that for most of the alloys with impurities situated to the left of the host cubic metals (Cu, Ag, and Au) in the Periodic Table there is a strong attraction between the probe In and the impurity atoms. This is in contrast to the situation for impurities to the right of the host metal Ag where repulsion was observed[1] as discussed in Ref. 3. The resulting large enhancement of the present impurity populations NN to the probe allowed us to study in detail different aspects of the impurity-probe interaction and of the EFG created by the impurity in the cubic host.

First we were able to follow in detail the onset of various NN configurations as the impurity concentration was increased. We have assumed that the lowest and first-appearing high frequency corresponds to a one NN impurity configuration. The other high frequencies appearing at higher concentrations were then successfully identified with configurations of more than one NN impurity on the basis of superpo-

sition of EFG's, thus confirming our interpretation. This kind of investigation of the EFG generated by impurities of known concentration can be of importance in interpreting the results of similar experiments concerned with defects generated by radiation damage and by ion implantation in metals. Moreover, the TDPAC technique is a microscopic tool giving important local information at the damaged site, in contrast to the majority of the investigations of radiation damaged metals which have been performed by macroscopic techniques.

For those alloys where temperature effects were studied, the high-frequency interaction was found to have the usual empirical $T^{3/2}$ dependence in all cases, supporting the idea of lattice vibrations as the cause of the temperature dependence. Further support for this came from a correlation between the parameter α, which gives the strength of the EFG temperature dependence, and the binding energy ΔE_B. This gave α smaller for the more strongly bound probe-impurity pairs. For the low frequencies, generated by non-NN impurities, departures from the $T^{3/2}$ dependence in parts of the temperature range occurred for some alloys. This is difficult to analyze because as the temperature varied not only the low frequency changed, but also its distribution. However, where the $T^{3/2}$ dependence was followed the obtained α was an order of magnitude larger than for the high-frequency interaction. This is expected as the binding between probe and non-NN impurities is much weaker than for NN impurities. It is interesting to compare our results with work on noncubic metals and on radiation damaged cubic metals. For ^{111}Cd in noncubic sp metals, where a strong attraction between probe and host atoms is not expected, the α parameters are large; they are of the same order of magnitude as we observed for the low frequencies. On the other hand, the temperature dependence of the EFG created by vacancies in cubic systems[18] is much weaker, giving $T^{3/2}$ slopes of the order of magnitude of those obtained for the NN high frequencies reported in the present paper.

The room-temperature high frequencies ν_h and the binding energies ΔE_B were analyzed on the basis of the differences in valence (ΔZ) and in period (λ) between the impurity and the host. The measured binding energies were augmented by making estimates of ΔE_B for those alloys where temperature effects were not studied. A smooth dependence of both the binding energy and the high frequency on ΔZ and λ was found. The dependence of ν_h on the period parameter λ can be interpreted as an effect of the electronic core of both the impurity and the matrix. Very probably this correlation evidences an effect related to the number of inner electrons in the atomic core. The increase of ν_h with ΔZ is in line with previous work for impurities to the right-hand side of the matrix in the Periodic Table.

It is interesting to compare our results with those obtained from NMR experiments. Most of the NMR work has been done in Cu matrix. Nevald and Petersen[19] measured the EFG's created by Ni, Pd, and Pt impurities in a single-crystal matrix of Cu. As discussed in Ref. 4, our result for the EFG acting on Cd in the CuPd alloy agrees very well with the value (also ascribed to one NN impurity) measured by NMR on Cu in the same alloy.[19] In the alloy of CuPt, Nevald and Petersen have not succeeded to detect NMR lines due to NN impurity; they found a low frequency which was attributed to next NN impurities and which gives an EFG of 0.21×10^{16} V/cm^2 after removing the probe dependence as usual by dividing by the Sternheimer factor. In the present experiment for CuPt we observe very clearly a high frequency due to one NN impurity and a low distributed frequency due to more distant impurities (see Fig. 1 and Table II), from which we extract EFG's of 1.4×10^{16} and 0.07×10^{16} V/cm^2, respectively. Considering the agreement of the results for CuPd it is difficult to understand why the EFG due to the NN Pt impurity was not observed in the NMR experiment, especially as the smaller-amplitude enhancement in CuPt would tend to make the TDPAC frequency determination, if anything less easy. Also our low distributed frequency is three times smaller than the NMR result, but one has to realize that the TDPAC technique is not able to resolve the contribution to the EFG from different non-NN shells.

In the present work we discuss our data from a phenomenological and systematic point of view, without a tentative interpretation of the EFG in terms of the existing models. The theoretical approach by Kohn and Vosko[20] and Blandin and Friedel[21] were able to account semiquantitatively for the "wipeout numbers" deduced from NMR experiments, by calculating the EFG produced by long-range oscillatory screening charge cloud surrounding the impurity atom. The situation is different in the case of an EFG generated by NN impurity atoms. The above model is not suitable for this situation, since it is an asymptotic model. More recent calculations have also failed in reproducing the currently existing data. The model used by Fukai and Watanabe[22] for Al-based alloys did not give the right order of magnitude, and calculations, performed for Cu-based alloys, not only do not give the order of magnitude, but also do not follow the systematics of the experimental results. Recently Sagalyn and Alexander[23] performed new calculations for the NMR data in Cu-based alloys, using a model which combines the valence effect and the size effect. They obtain good fittings to the experimental results, concluding that the size effect is responsible for as much as 40% of the EFG in some alloys. The difficulty with this approach is that the used EFG-strain coupling constant required to account for the data is much larger

than the constant inferred from experiments on plastically deformed pure Copper. It seems that we need more elaborate theoretical models in order to understand better the mechanism responsible for the EFG and also for the impurity-probe binding in doped cubic metals.

*Present address: Comision Nacional de Energia Atómica, Buenos Aires, Argentina.

†On leave from Universidad Nacional de La Plata and CONICET, Argentina, under the exchange program CNPq-CONICET.

[1] R. P. Livi, M. Behar, and F. C. Zawislak, Hyper. Inter. 5, 1 (1977).

[2] J. A. H. da Jornada, L. Amaral, I. J. R. Baumvol, M. Behar, R. P. Livi, and F. C. Zawislak, Phys. Lett. A 64, 246 (1977).

[3] J. A. H. da Jornada, I. J. R. Baumvol, M. Behar, R. P. Livi, and F. C. Zawislak, Hyper. Inter. 5, 219 (1978).

[4] I. J. R. Baumvol, M. Behar, J. A. H. da Jornada, E. R. Fraga, R. P. Livi, and F. C. Zawislak, J. Phys. F 9, 1233 (1979).

[5] K. Królas, K. Parliński, B. Wodniecka, and P. Wodniecki, Hyper. Inter. 4, 600 (1978).

[6] K. Królas, B. Wodniecka, and P. Wodniecki, Hyper. Inter. 4, 605 (1978).

[7] M. Hansen, Constitution of Binary Alloys, 2nd ed. (McGraw-Hill, New York, 1958).

[8] R. P. Elliott, Constitution of Binary Alloys, 1st Suppl. (McGraw-Hill, New York, 1965).

[9] H. Frauenfelder and R. M. Steffen, in Alpha-, Beta- and Gamma-Ray Spectroscopy, edited by K. Siegbahn (North-Holland, Amsterdam, 1965), Vol. 2, p. 997.

[10] J. Christiansen, P. Heubes, R. Keitel, W. Klinger, W. Loeffler, W. Sandner, and W. Witthuhn, Z. Phys. B 24, 177 (1976).

[11] P. Jena, Phys. Rev. Lett. 36, 418 (1976).

[12] K. Nishiyama, F. Dimmling, Th. Kornrumpf, and D. Riegel, Phys. Rev. Lett. 37, 357 (1976).

[13] M. D. Thompson, P. C. Pattnaik, and T. P. Das, Phys. Rev. B 18, 5402 (1978).

[14] I. J. R. Baumvol, M. Behar, J. R. Iglesias-Sicardi, R. P. Livi, and F. C. Zawislak, Phys. Rev. B 18, 6713 (1978).

[15] J. R. Iglesias-Sicardi, Phys. Lett. A 64, 406 (1978).

[16] A. O. E. Animalu, Phys. Rev. B 8, 3542 (1973).

[17] R. Nevald, B. L. Jensen, and P. B. Fynbo, J. Phys. F 4, 1320 (1974).

[18] A. Weidinger, O. Echt, E. Recknagel, G. Schatz, and Th. Wichert, Phys. Lett. A 65, 247 (1978).

[19] R. Nevald and G. Petersen, J. Phys. F 5, 1778 (1975).

[20] W. Kohn and S. H. Vosko, Phys. Rev. 119, 912 (1960).

[21] A. Blandin and J. Friedel, J. Phys. Radium 21, 689 (1960).

[22] Y. Fukai and K. Watanabe, Phys. Rev. B 10, 3015 (1974).

[23] P. L. Sagalyn and M. N. Alexander, Phys. Rev. B 15, 5581 (1977).